



HAL
open science

Experimental study on the influence of holes on the transition on an incompressible boundary layer

Jeanne Methel, Delphine Sebbane, Maxime Forte, Olivier Vermeersch

► To cite this version:

Jeanne Methel, Delphine Sebbane, Maxime Forte, Olivier Vermeersch. Experimental study on the influence of holes on the transition on an incompressible boundary layer. AERO2022 - 56th 3AF International Conference on Applied Aerodynamics, Mar 2022, Toulouse, France. hal-03772583

HAL Id: hal-03772583

<https://hal.science/hal-03772583>

Submitted on 8 Sep 2022

HAL is a multi-disciplinary open access archive for the deposit and dissemination of scientific research documents, whether they are published or not. The documents may come from teaching and research institutions in France or abroad, or from public or private research centers.

L'archive ouverte pluridisciplinaire **HAL**, est destinée au dépôt et à la diffusion de documents scientifiques de niveau recherche, publiés ou non, émanant des établissements d'enseignement et de recherche français ou étrangers, des laboratoires publics ou privés.

Experimental study on the influence of holes on the transition on an incompressible boundary layer

Jeanne Methel⁽¹⁾, Delphine Sebbane⁽²⁾, Maxime Forte⁽³⁾ and Olivier Vermeersch⁽⁴⁾

⁽¹⁾ONERA/DMPE, Université de Toulouse, Toulouse 31055, France, jeanne.methel@onera.fr

⁽²⁾ONERA/DMPE, Université de Toulouse, Toulouse 31055, France, delphine.sebbane@onera.fr

⁽³⁾ONERA/DMPE, Université de Toulouse, Toulouse 31055, France, maxime.forte@onera.fr

⁽⁴⁾ONERA/DMPE, Université de Toulouse, Toulouse 31055, France, olivier.vermeersch@onera.fr

28 March 2022

ABSTRACT

In the present experimental study, the effect of holes on the transition of an incompressible boundary layer was investigated. Two configurations of the symmetric profile ONERA-D at a fixed angle of attack were tested: one with zero-, and the other with 60°-sweep angle. These two configurations enabled to study the interaction of holes with either a highly stable (no sweep) or unstable (with sweep) boundary layer. Overall, although some differences between configurations were observed, the main findings from this study were applicable to both. In particular, no gradual upstream shift in transition position occurred as either hole diameter d or depth h were varied: once critical dimensions (for which transition position was immediately downstream of the hole) were reached, transition abruptly moved from the baseline location to that of the hole. Next, characterising hole geometry using the aspect ratio h/d proved to be useful in determining a threshold across which boundary layer sensitivity to holes was modified. Finally, holes with $h/\delta_1 \geq 2$, and $d/\delta_1 \geq 25$ tended to trigger transition immediately downstream of their location.

1. INTRODUCTION

Aircraft fuel consumption can be significantly reduced by decreasing skin-friction drag of lifting surfaces through laminar-turbulent transition delay. One approach is to design airfoil profile geometries that use favourable pressure gradients to stabilise the boundary layer: the result is Natural Laminar Flow (NLF) profiles. Although us-

ing profile geometry to achieve a desired performance is not new, improvements in both the design tool chain and the manufacturing process allow NLF profiles with large extents of laminar flow to be considered as serious candidates for commercial applications.

In this context, manufacturing tolerances need to be defined for NLF profiles to be considered commercially viable. Numerous investigations, both numerical and experimental, exist on the effect on transition of two-dimensional defects, such as backward- and forward-facing steps ([21], [20], [14], [15]), rectangular gaps ([16], [4], [22]) or bumps ([8], [9], [5]). Based on these results, empirical criteria, often based on the defect dimensions and the local boundary layer thickness at the defect location, ([10], [1]) and models ([2], [3]) were developed. Similar studies exist for three-dimensional defects, such as isolated roughness elements of different cross-sections ([7], [19] [17] or [12]). However, the equivalent work on holes is not currently available in the open literature.

In low freestream turbulence environments, the natural path to transition, according to [13], occurs. Disturbances from the freestream penetrate the boundary layer through the receptivity process and excite its primary modes. These modes can then undergo a region of linear amplification, which can be modelled using Linear Stability Theory; however, past a threshold amplification, secondary instabilities develop, quickly leading to the occurrence of the first turbulent spot, which heralds the onset of transition. In the following paragraphs, transition governed by crossflow (CF) instabilities is described in a boundary layer assumed to be developing in a low

freestream turbulence level.

In three-dimensional flow, such as a swept wing, the primary modes (CF instabilities) are co-rotating vortices that are amplified and aligned with the freestream direction. These CF instabilities tend to undergo stronger amplification in accelerated flow (negative pressure gradient), as opposed to two-dimensional flow that is stabilised under these conditions. Additionally, because of the alignment of the CF instabilities, the transition front has a saw-tooth pattern that corresponds to variations in the local amplification of individual CF vortices. These variations can typically occur as a result of localised surface roughness or defects, to which CF instabilities are highly receptive, as shown, both experimentally and numerically, by [12], [6], [18].

The purpose of the present study is therefore to provide some empirical criteria on the effects on laminar-turbulent transition of holes. Given the different behaviour of an accelerated boundary layer in two- or three-dimensional flow, the experimental investigation was performed on an ONERA-D symmetric profile, with holes near its leading edge, tested at two different sweep angles (zero and 60°). Additionally, the profile's angle of attack was set so as to achieve accelerated flow on the suction side.

In the first section of this paper, the experimental facility, including the ONERA-D profile and surface defect inserts used, are described. In the next section, the effects of holes on laminar-turbulent transition of the unswept profile are discussed, followed by a similar discussion for the swept profile. Empirical criteria are then proposed based on the combined results from the unswept and swept configurations.

2. EXPERIMENTAL METHOD

In this section, the experimental facility and airfoil model used for this investigation are described. The instrumentation used, mainly hot-wire anemometry, is presented, along with the procedure to characterise the effect of holes on boundary layer transition.

2.1 Experimental facility and model

This experimental investigation was conducted in the ONERA TRIN1 subsonic wind tunnel, an open-return facility operating at atmospheric conditions. Achievable freestream velocities at the test section entrance range from $5 \text{ m}\cdot\text{s}^{-1}$ to $80 \text{ m}\cdot\text{s}^{-1}$, and the corresponding freestream turbulence levels, evaluated over the frequency band 50 Hz to 10 kHz, are between 0.05% and 0.15%. In the present study, freestream velocities did not exceed $60 \text{ m}\cdot\text{s}^{-1}$. At the inlet of the test section, dimensions are 0.35 m by 0.6 m (height x width). Over the 2.5 m of length of the test section, the ceiling and

floor walls slightly diverge to account for the thickening of their boundary layers.

The ONERA-D symmetric profile used for this study has a chord length, c , of 0.35 m and a span, s , of 2 m. Between the leading edge and 40% of the chord, fifteen pressure taps allow monitoring of the pressure distribution. The wing section is mounted horizontally at mid-height of the test section, as shown in Figure 1 and its angle of attack α was set to -8° (negative angle is pitching down) to obtain continuously accelerated flow on the upper (suction) side of the model.

With this angle of attack fixed, two configurations were then tested. First, the two-dimensional configuration where the sweep angle of the model was set to 0° , such that transition was governed by TS instabilities. As mentioned previously, these instabilities are considered stable, being in a constantly accelerated flow on the suction side, as shown on the pressure coefficient distributions in red on Figure 2. As an illustration of this stable nature of the flow, the transition position was determined at $x/c = 0.9$ during a previous campaign at the same angle of attack and at a freestream velocity of $75 \text{ m}\cdot\text{s}^{-1}$. Flow is therefore laminar and extremely stable at the location of the inserts ($x/c = 0.1$) across the range of freestream velocities presently tested.

Secondly, the three-dimensional configuration had the profile mounted with a 60° sweep angle in order to promote transition governed by CF instabilities. In this case, the combination of accelerated flow (as shown in blue on Figure 2) and CF instabilities results in an unstable case. Based on previous experiments on this identical configuration, the transition position was thus found to be upstream of the unswept case. In particular, the transition position moved from $x/c = 0.7$ for a freestream velocity $U_\infty = 30 \text{ m}\cdot\text{s}^{-1}$ to $x/c = 0.26$ at $U_\infty = 70 \text{ m}\cdot\text{s}^{-1}$. However, and similar to the unswept configuration, flow is laminar, but unstable, at the defect and hot-wire probing locations.

As a note, although only fifteen pressure taps are available on the current model, another ONERA-D model, tested in 1997, was instrumented with pressure taps along its entire chord. The pressure coefficient distribution from this past campaign, at the same angle of attack and sweep angles, are provided over the entire chord on the upper side as reference on Figure 2.

A metallic insert in the leading edge of the model was fitted with a 160 mm-long metallic slot (in the spanwise direction) that allowed to test a row of five holes at 10% chord of the upper side, as shown in Figure 1. To avoid interaction between the different holes, especially in the swept configuration, a minimum distance of 35 mm between each hole was established. A set of 10 different metallic slots were tested for a total of 50 different cylindrical hole geometries. Hole depth h ranged from $300 \mu\text{m}$ to $1200 \mu\text{m}$ and diameter d from 1 mm to 8 mm. Verification measurements were performed, and showed that

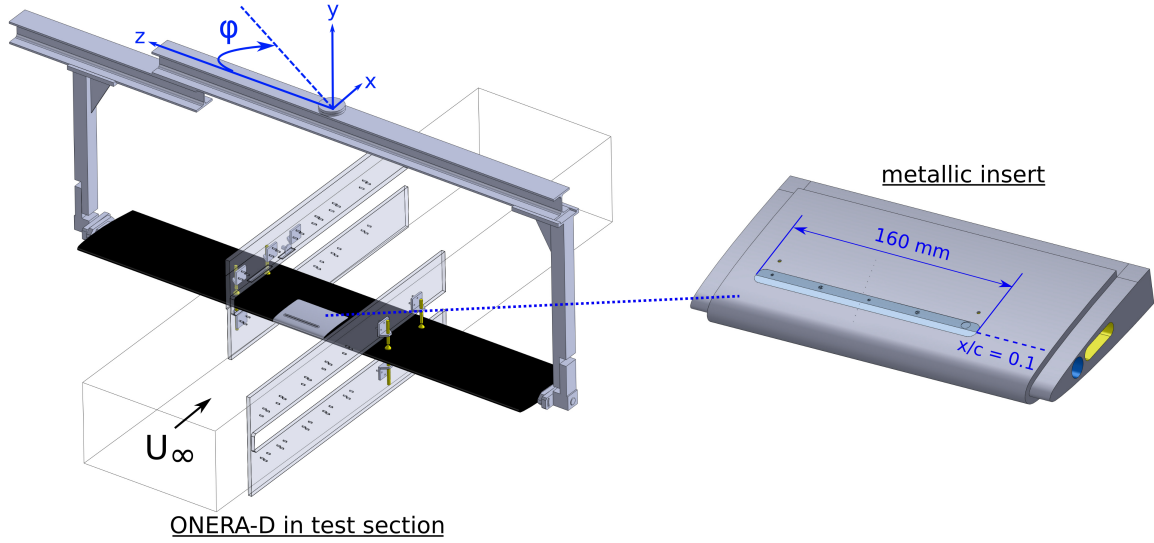


Figure 1: Overview of the ONERA-D mounted in the test section with a detailed view of the leading edge metallic insert with a 5-hole slot.

actual hole depth was within $\pm 15 \mu\text{m}$ from design intent. For purposes of clarity, hole depths will be referred to by their design intent.

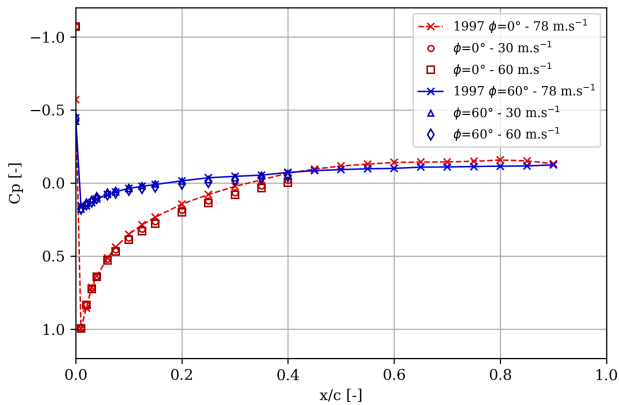


Figure 2: Pressure coefficient distribution over the ONERA-D at α set to -8° for both unswept ($\phi = 0^\circ$) and swept ($\phi = 60^\circ$) configurations on the upper side.

2.2 Instrumentation

Velocity measurements in the boundary layer were performed using constant temperature hot-wire anemometry (Dantec Streamline with a 90C10 CTA module and Dantec 55P15 single-wire probes). After A/C coupling, the signal from the hot-wire is low-pass filtered at 4 kHz according to the Nyquist's law, and amplified with a gain of 10 to maximise the input range of the A/D converter. The

sampling frequency was set to 10 kHz. These sampling and anti-aliasing frequencies were increased to 25 kHz and 10 kHz respectively for specific measurements, such as spectral analysis.

To characterise the effect of a hole on boundary layer transition, velocity fluctuations at a fixed location downstream of any given hole were acquired. A non-calibrated hot-wire probe was used, positioned at a constant distance from the upper surface ($y = 250 \mu\text{m}$), and freestream velocity U_∞ was gradually increased. Since the hot-wire is fixed and usually close to the surface defect position, a critical unit Reynolds number (based on freestream velocity and ambient air density and viscosity) was determined for each defect. Note that, in the remainder of this paper, hot-wire measurements will only be given in root mean square (rms) of a voltage, since the probe was not calibrated; however, voltage fluctuations are directly related to freestream velocity fluctuations. The critical unit Reynolds number is therefore a function of the ambient air conditions and the freestream velocity at which the velocity fluctuations start to increase, thereby indicating the onset of transition at the position of the hotwire.

3. EXPERIMENTAL CHARACTERISATION OF THE EFFECT OF HOLES ON TRANSITION

In the following section, the effect of individual hole parameters (i.e., diameter and depth) on transition is investigated for both configurations. Critical dimensions are then determined to provide some guidelines on hole parameter dimensions that minimise the effect on transition

in a subsonic boundary layer.

3.1 Effect of holes in the unswept configuration

Hole diameter was investigated for a range of hole depths. For the zero-sweep configuration, two main behaviours depending on the hole aspect ratio h/d were identified, and are illustrated with the chosen depths of h equal to $400\ \mu\text{m}$ and $1000\ \mu\text{m}$ in Figure 3. The figure shows the evolution of voltage fluctuations recorded by the hotwire (located at the x/c indicated in the legend) as freestream velocity U_∞ is increased. The unit Reynolds number Re_u based on ambient air conditions and U_∞ is also indicated. The critical parameters $U_{\infty,c}$ and $Re_{u,c}$ then correspond to the conditions for which hotwire fluctuations started to increase, indicating the presence of the first turbulence spots and thus the onset of transition. For example, the 3 mm-diameter hole with depth h equal to $400\ \mu\text{m}$ in Figure 3 has $U_{\infty,c}$ equal to $54\ \text{m s}^{-1}$ or $Re_{u,c}$ equal to $3.6 \cdot 10^6$.

In Figure 3 and for the 6-mm diameter hole, the hotwire location downstream of the hole was varied between 13% and 20% of the chord to evaluate the influence of probing position on the identification of the critical unit Reynolds number (and critical freestream velocity). In both cases, the critical unit Reynolds number $Re_{u,c}$ is approximately $3.65 \cdot 10^6$, indicating that transition moves abruptly from the reference (smooth case) position to the surface defect position. The transition position therefore does not gradually shift towards the hole location as freestream velocity is increased. This result is typical of three-dimensional surface defects, which introduce three-dimensional effects and promote the breakdown to turbulence of the boundary layer instabilities. On the other hand, this behaviour is different from subcritical two-dimensional surface defects such as gaps or steps that have a more gradual effect on transition position shift.

As a note, in the present investigation, defects are considered subcritical when, under their influence, the transition position gradually moves between the smooth reference configuration and the defect location. Consequently, defects are considered critical when the transition position is immediately downstream of the surface defect. As a reminder, all holes tested in this study are located at 10% chord. Therefore, the increase in streamwise velocity fluctuations measured by the hotwire at 13% chord indicates that transition occurs close enough to the hole position to consider that the hole is critical for the given freestream flow condition.

Additionally, Figure 3 shows that across the range of tested wind tunnel velocities and at the chosen hole depth h of $400\ \mu\text{m}$, diameter does not seem to affect $Re_{u,c}$, which is approximately $3.65 \cdot 10^6$ for all cases. On the other hand, considering cases where h is set to $1000\ \mu\text{m}$,

hole diameter has a significant effect on $Re_{u,c}$. As hole diameter increases, the $Re_{u,c}$ decreases. The main difference seems to be that for the data set with h equal to $400\ \mu\text{m}$, all holes had an aspect ratio h/d less than 0.2, whereas the data set with h equal to $1000\ \mu\text{m}$ had holes with an aspect ratio greater than 0.2, as shown by the filled symbols.

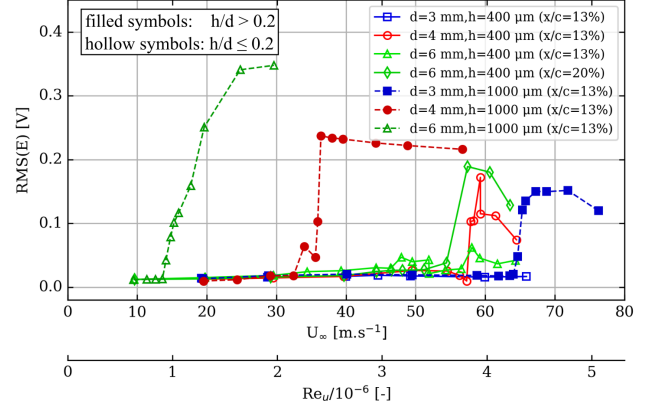


Figure 3: Variation in critical Reynolds number with hole diameter for two chosen depths and probing location for the unswept configuration ($\phi = 0^\circ$).

Next, the effect of hole depth is investigated for a selection of two diameters, and shown in Figure 4. For the smallest diameter, d equal to 3 mm, a non-monotonic behaviour in the $Re_{u,c}$ can be observed. In particular, as hole depth increases between $400\ \mu\text{m}$ and $600\ \mu\text{m}$, $Re_{u,c}$ decreases, indicating that, as can be intuitively expected, deeper holes tend to promote transition. However, as hole depth further increases to values of $800\ \mu\text{m}$, $Re_{u,c}$ starts to increase again to such an extent that the deepest hole such that $h = 800\ \mu\text{m}$ has a greater $Re_{u,c}$ than the shallow hole $h = 600\ \mu\text{m}$. The hole dimensions ($d = 3\ \text{mm}$, $h = 600\ \mu\text{m}$) for which the change of behaviour occurs, and therefore where the minimum $Re_{u,c}$ can be found, actually corresponds to an aspect ratio of 0.2.

Figure 4 also shows holes that all have d equal to 6 mm, and aspect ratios less than or equal to 0.2. For this range of aspect ratios, a single trend can be observed where an increase in hole depth corresponds to a decrease in $Re_{u,c}$.

Overall, in the zero sweep configuration, the boundary layer is extremely stable, and shows greatest sensitivity to holes with an aspect ratio h/d close or equal to 0.2. Additionally, for holes with an aspect ratio less than 0.2, diameter was not an influencing parameter. Similar to three-dimensional positive surface defects, there are no intermediate transition positions between a smooth (or subcritical) case and a critical case. The transition position abruptly moves from the reference smooth case location to the hole location once critical hole dimensions are reached.

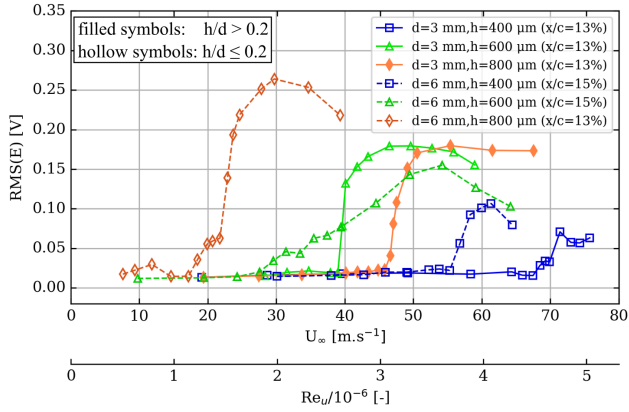


Figure 4: Variation in critical Reynolds number with hole depth for two chosen diameters for the unswept configuration ($\phi = 0^\circ$)

3.2 Effect of holes in the swept configuration

The effects of hole diameter and depth on the boundary layer transition in the swept configuration are now investigated, using the same hole geometries as those in the previous section.

Figure 5 shows the effect of hole diameter for depths 400 μm and 1000 μm . In particular, the critical Reynolds number $Re_{u,c}$ for 4-mm diameter hole is determined at different probing locations downstream of the hole, 13% to 19% of chord. Similar to the unswept configuration, $Re_{u,c}$ remains relatively constant regardless of the probing location, in the present case close to $4 \cdot 10^6$. The transition position therefore abruptly moves from the smooth case position to one immediately downstream of the hole in the swept configuration, where the transition mechanism is governed by crossflow instabilities.

Additionally, regardless of hole aspect ratio, Figure 5 shows that, as hole diameter increases, $Re_{u,c}$ decreases. Therefore, for any tested hole depth, a larger hole diameter leads to earlier transition. However, as a note, the most destabilising (i.e., with lowest $Re_{u,c}$) hole geometry for the 1000 μm -deep hole is that with an aspect ratio relatively close to 0.2: the 6-mm diameter hole, with its corresponding h/d equal to 0.167.

Next, Figure 6 shows the effect of varying depth for 3 mm- and 6 mm-diameter holes. For the 3-mm diameter holes (solid lines) with h/d less than 0.2 (unfilled symbols), increasing depth corresponds to a reduction in $Re_{u,c}$. In particular, the hole with a depth of 400 μm ($h/d = 0.133$) does not trigger transition over the range of the freestream velocities achievable by the present wind tunnel facility. The lowest value of $Re_{u,c}$, equal to $4.3 \cdot 10^6$, is reached for the hole with h/d equal to 0.2, with its 3-mm diameter and 600 μm depth. As hole depth is further increased to 800 μm , the aspect ratio becomes greater than

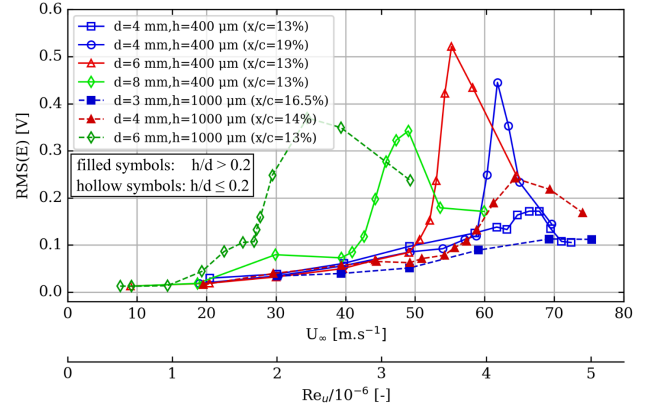


Figure 5: Variation in critical Reynolds number with hole diameter and probing location for the swept configuration ($\phi = 60^\circ$)

0.2, and the $Re_{u,c}$ then starts to increase back to values outside the range of the wind tunnel facility. For the 6 mm-diameter holes, only aspect ratios less than 0.2 could be tested. In this case, increasing depth destabilises the boundary layer and results in lower $Re_{u,c}$.

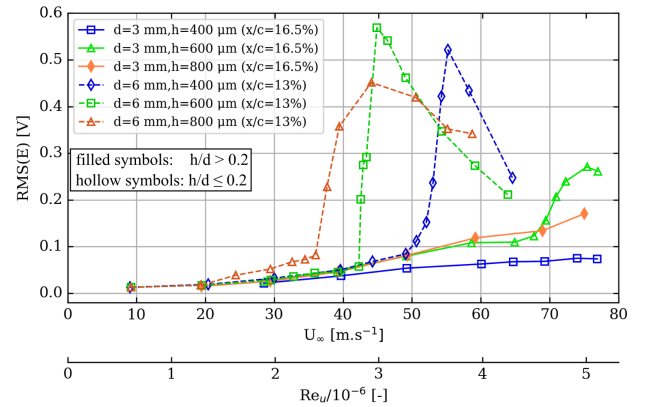


Figure 6: Variation in critical Reynolds number with hole depth for the swept configuration ($\phi = 60^\circ$)

In the swept configurations, regardless of aspect ratio, increasing either hole depth or diameter led to a change in $Re_{u,c}$, indicating a modification in boundary layer stability. However, a minimum $Re_{u,c}$ occurred for holes having an aspect ratio of 0.2, exhibiting a similar behaviour to the unswept configuration.

3.3 Critical dimensions

In the previous sections, the effect of individual parameters, such as depth and diameter, were investigated for both the unswept and swept configurations in terms of the evolution of critical freestream velocity or unit Reynolds number. The present section now focuses on establishing

a more general overview of the effect of hole geometries by using local parameters. In particular, the depth-based Reynolds number, Re_d is defined as:

$$Re_d = \frac{u_{e,c}d}{\nu} \quad (1)$$

with $u_{e,c}$ defined as the boundary layer edge velocity at the hole location ($x/c = 10\%$) for the critical freestream velocity $U_{\infty,c}$. As mentioned earlier, for the unswept configuration, u_e/U_{∞} is equal to 0.76. For the 60° -sweep configuration, u_e/U_{∞} is 0.975.

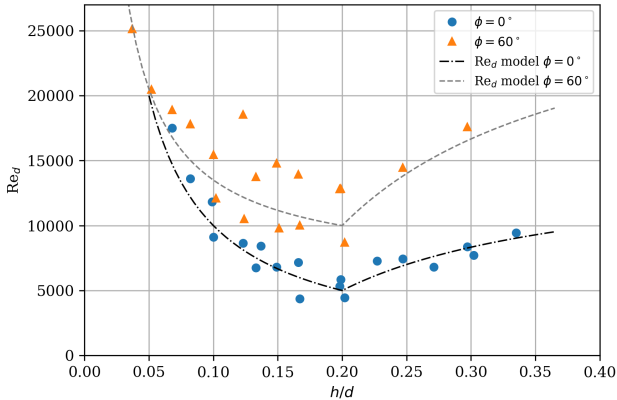
Figure 7 shows the evolution of Re_d as a function of aspect ratio h/d , for both sweep configurations. Regardless of sweep angle or dimension used to define the Reynolds number, the aspect ratio value of 0.2 emerges as a parameter of interest. In particular, at this h/d value, Re_d reaches a minimum, albeit different depending on sweep configuration. Proposed models for the evolution of Re_h as a function of h/d are, for the unswept configuration:

$$Re_d = \begin{cases} 1000 \frac{d}{h}, & \text{for } h/d < 0.2 \\ 15000 - 2000 \frac{d}{h}, & \text{for } h/d > 0.2 \end{cases} \quad (2)$$

and for the swept configuration:

$$Re_d = \begin{cases} 6500 + 700 \frac{d}{h}, & \text{for } h/d < 0.2 \\ 30000 - 4000 \frac{d}{h}, & \text{for } h/d > 0.2. \end{cases} \quad (3)$$

These simple models are proposed in the present context because of the single sweep angle that was tested. Authors are aware that a more adequate model would include sweep angle information. Additionally, the models for Re_h are obtained by the relationship with Re_d such that $Re_d = Re_h \cdot (d/h)$.



(a) Re_d vs. h/d

Figure 7: Diameter-based Reynolds number as a function of aspect ratio h/d

Another synthetic representation of critical hole dimensions is shown in Figure 8, where the critical hole

depth and diameter are non-dimensionalised by the local displacement thickness δ_1 . This δ_1 value was calculated using ONERA's in-house boundary layer code. In Figure 8, the shaded region corresponds to cases for which the combination of h/δ_1 and d/δ_1 do not trigger transition and the boundary layer is laminar at the hole location. However, combining results from both sweep configurations, an L-shaped curve, similar to that of [11] (available in the open literature in [1]), emerges. In general, the conjunct criteria necessary for a hole to trigger transition can be estimated to be approximately $h/\delta_1 \geq 1$, and $d/\delta_1 \geq 15$.

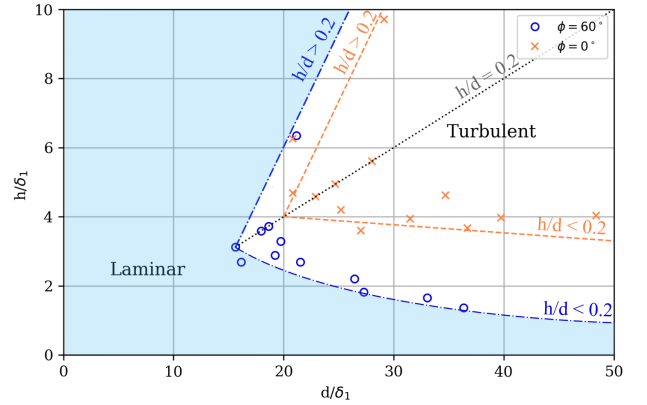


Figure 8: Conjunct critical parameters (normalized depth h/δ_1 and diameter d/δ_1) for tested isolated holes. Green-shaded region represents defects for which laminar flow is maintained and no-shading is where defects are critical. Branches correspond to holes with aspect ratio h/d greater and less than 0.2, as labelled.

4. CONCLUSION

An experimental study on the effect of holes on the transition of an incompressible boundary layer was performed. Two sweep angles were tested to investigate the response of a boundary layer in stable (zero sweep configuration) and unstable (60° sweep) conditions. Holes were located at 10% chord and their effect was determined in terms of critical freestream velocity $U_{\infty,c}$ or unit Reynolds number $Re_{u,c}$. Based on these freestream parameters, local boundary layer parameters at the hole location, such as boundary layer edge velocity u_e and displacement thickness δ_1 , were determined to define local Reynolds numbers based on either hole depth or diameter. First, various probing locations downstream of the same hole resulted in relatively similar $Re_{u,c}$, indicating that transition moved abruptly from the reference (smooth case) transition position to the hole location. Next, for both sweep configurations, a change in the evolution of either Re_h or Re_d occurred at h/d 0.2. This hole aspect ratio there-

fore seems to particularly destabilise the incompressible boundary layer presently investigated. Finally, conjunct critical parameters were determined based on data from both sweep configuration, similar to those for gaps. In particular, holes with $h/\delta_1 \geq 1$, and $d/\delta_1 \geq 15$ tend to trigger transition immediately downstream of their location.

5. ACKNOWLEDGMENTS

Work presented in this paper was performed within the Joint Technology Initiative *JTI Clean Sky*, Smart Fixed Wing Aircraft Integrated Technology Demonstrator SFWAITD project (contract N° CSJU-GAM-SFWA-2008-001) financed by the 7th Framework Program of European Commission.

REFERENCES

- [1] S. Béguet, J. Perraud, M. Forte, and J.-Ph. Brazier. Modeling of transverse gaps effects on boundary-layer transition. *Journal of Aircraft*, 54(2):794–801, 2016.
- [2] J. Crouch, V. Kosorygin, and L. Ng. Modeling the effects of steps on boundary-layer transition. In *IUTAM Symposium on Laminar-Turbulent Transition*, pages 37–44. Springer, 2006.
- [3] J. Crouch, V. Kosorygin, and M. Sutanto. Modeling gap effects on transition dominated by tollmien-schlichting instability. In *AIAA AVIATION 2020 FORUM*, page 3075, 2020.
- [4] M. Forte, L. Gentili, S. Béguet, J. Perraud, and G. Casalis. Experimental and numerical study of the effect of gaps on the laminar-turbulent transition for two-dimensional incompressible boundary-layers. In *50th 3AF International Conference on Applied Aerodynamics*, 2015.
- [5] J. Franco Sumariva and S. Hein. Adaptive Harmonic Linearized Navier-Stokes equations used for boundary-layer instability analysis in the presence of large streamwise gradients. *2018 Aerospace Sciences Meeting, AIAA Scitech Forum*, 2018.
- [6] V. Gaponenko, A. Ivanov, Y. Kachanov, and J. Crouch. Swept-wing boundary-layer receptivity to surface non-uniformities. *Journal of Fluid Mechanics*, 461:93–126, 2002.
- [7] N. Gregory and W. Walker. *The effect on transition of isolated surface excrescences in the boundary layer*. Aeronautical Research Council, 1956.
- [8] P. Klebanoff and K. Tidstrom. Mechanism by which a two-dimensional roughness element induces boundary-layer transition. *The Physics of Fluids*, 15(7):1173–1188, 1972.
- [9] A. Nayfeh, S. Ragab, and J. Masad. Effect of a bulge on the subharmonic instability of boundary layers. *Physics of Fluids A: Fluid Dynamics*, 2(6):937–948, 1990.
- [10] J. Nenni and G. Gluyas. Aerodynamic design and analysis of an LFC surface. *Astronautics & Aeronautics*, 4(7):52, 1966.
- [11] M. Olive and A. Blanchard. Etude expérimentale du déclenchement de la transition par des cavités en écoulement incompressible. Technical report, CERT DERAT OA18/5007, 1982.
- [12] R. Radeztsky Jr, M. Reibert, and W. Saric. Effect of isolated micron-sized roughness on transition in swept-wing flows. *AIAA journal*, 37(11):1370–1377, 1999.
- [13] E. Reshotko. Paths to transition in wall layers. *Papers presented during the AVT-151 RTO AVT/VKI Lecture Series held at the von Kármán Institute, Rhode St. Gense, Belgium*, pages 9–12, 2008.
- [14] A. Rius-Vidales and M. Kotsonis. Influence of a forward-facing step surface irregularity on swept wing transition. *AIAA Journal*, 58(12):5243–5253, 2020.
- [15] S. Sinha, A. Gupta, and M. Oberai. Laminar separating flow over backsteps and cavities. I-backsteps. *AIAA Journal*, 19(12):1527–1530, 1981.
- [16] S. Sinha, A. Gupta, and M. Oberai. Laminar separating flow over backsteps and cavities. II-cavities. *AIAA Journal*, 20(3):370–375, 1982.
- [17] I. Tani. Effect of two-dimensional and isolated roughness on laminar flow. In G.V. Lachmann, editor, *Boundary Layer and Flow Control*, pages 637–656. Pergamon, 1961.
- [18] D. Tempelmann, L.-U. Schrader, A. Hanifi, L. Brandt, and D. Henningson. Swept wing boundary-layer receptivity to localized surface roughness. *Journal of Fluid Mechanics*, 711:516–544, 2012.
- [19] A. von Doenhoff and A. Braslow. The effect of distributed surface roughness on laminar flow. In *Boundary layer and flow control*, pages 657–681. Elsevier, 1961.
- [20] Y. Wang and M. Gaster. Effect of surface steps on boundary layer transition. *Experiments in Fluids*, 39(4):679–686, 2005.

- [21] A. Wörner, U. Rist, and S. Wagner. Humps/steps influence on stability characteristics of two-dimensional laminar boundary layer. *AIAA Journal*, 41:192–197, 2003.
- [22] J. Zahn and U. Rist. Impact of deep gaps on laminar–turbulent transition in compressible boundary-layer flow. *AIAA Journal*, 54(1):66–76, 2015.